Letter

Lattice simulations of the QCD chiral transition at real baryon density

Szabolcs Borsányi,[1] Zoltán Fodor,[1,2,3,4,5] Matteo Giordano,[4] Sándor D. Katz,[4,6] Dániel Nógrádi,[4] Attila Pásztor,[4,*] and Chik Him Wong[1]

[1]*Department of Physics, Wuppertal University, Gaussstr. 20, D-42119 Wuppertal, Germany*
[2]*Pennsylvania State University, Department of Physics, State College, Pennsylvania 16801, USA*
[3]*Jülich Supercomputing Centre, Forschungszentrum Jülich, D-52425 Jülich, Germany*
[4]*ELTE Eötvös Loránd University, Institute for Theoretical Physics, Pázmány Péter sétány 1/A, H-1117 Budapest, Hungary*
[5]*Physics Department, UCSD, San Diego, California 92093, USA*
[6]*MTA-ELTE Theoretical Physics Research Group, Pázmány Péter sétány 1/A, H-1117 Budapest, Hungary*

(Received 14 September 2021; accepted 4 February 2022; published 22 March 2022)

We use the sign-reweighting method to simulate the QCD chiral transition at real baryon densities on phenomenologically relevant lattices. This avoids the severe limitations of extrapolating from zero or imaginary chemical potential and the overlap problem of traditional reweighting approaches, opening up a new window to reliably study hot and dense strongly interacting matter from first principle lattice simulations. We demonstrate that sign reweighting can reach up to a baryochemical potential-temperature ratio of $\mu_B/T = 2.7$, covering most of the Relativistic Heavy Ion Collider Beam Energy Scan range.

DOI: 10.1103/PhysRevD.105.L051506

I. INTRODUCTION

The properties of strongly interacting matter at high temperature and density play a role in a variety of issues, such as the early history of the Universe and the scattering of heavy ions. These issues are currently at the center of intense theoretical and experimental investigations, and a deeper understanding of hot and dense strongly interacting matter would greatly help in furthering progress. In particular, the chiral transition has garnered a lot of interest [1–16], as the comparison of theoretical predictions with results from heavy-ion experiments can potentially challenge our understanding of strong interactions based on QCD. It is therefore important to obtain predictions for the behavior of strongly interacting matter near the chiral transition starting from first principles.

The most well-established method for first-principles studies of QCD in the strongly coupled regime near the transition is lattice QCD [17]. The lattice approach turns the path integral of quantum field theory into a practical numerical method by mapping it to a statistical-mechanics system. This method can in principle be systematically improved to reach arbitrary accuracy. Indeed, many aspects of QCD thermodynamics have been clarified using this method, such as the crossover nature of the transition and the value of the transition temperature at zero baryon density [4–6]. A timely challenge is then a lattice calculation of the properties of matter at finite density, such as the location of the critical end point—predicted by effective and functional approaches [7–10]. QCD at finite density is, however, not amenable to first-principle lattice studies using standard techniques, since in this case the Boltzmann weights in the path integral representation are complex and so not suitable for importance-sampling algorithms. A variety of methods have been proposed over the years to sidestep this complex action problem. None of these methods is, however, completely satisfactory, as they all suffer from systematic effects of some kind. Methods based on using an imaginary chemical potential [14,18–35] or a Taylor expansion around vanishing chemical potential [11,36–48] involve a certain amount of modeling, as they necessarily make assumptions about the functional dependence of physical observables on the chemical potential, in order to reconstruct them at real, finite chemical potential. Despite its formal exactness, the overlap problem when reweighting from zero chemical potential $\mu_B = 0$ [49–54] makes it very difficult to quantify statistical and systematic uncertainties. This is also true for the complex Langevin approach [55–61] due to its convergence issues. Yet, other speculative methods, such as dual variables [62,63] or Lefshetz thimbles [64–68] have only been successfully used to study toy models so far.

*Corresponding author:
apasztor@bodri.elte.hu

Although technically manifesting as different, the analytic continuation problem of the Taylor and imaginary chemical potential methods and the overlap problem of reweighting from $\mu_B = 0$ have the same origin: an inability to directly sample the gauge configurations most relevant to finite-density QCD, thus requiring an extrapolation that hopefully captures the features of the theory of interest. One would instead like to perform simulations in a theory from which reconstruction of the desired theory is the least affected by systematic effects, by (*i*) keeping as close as possible to the most relevant configurations, thus minimizing the overlap problem, and (*ii*) making the complex-action problem, or sign problem, due to cancellations among contributions, as mild as possible. A method satisfying both requirements—"sign reweighting"—has sporadically been mentioned in the literature for quite some time [69–75]. Moreover, sign reweighting is the optimal choice, with the weakest sign problem, out of reweighting schemes based on simulating theories where the Boltzmann weights differ from the desired ones only by a function of the phase of the quark determinant [69–71]. This approach is so far the closest one can get to sampling the most relevant configurations according to the original, sign-problem-ridden path integral and allows one to answer detailed questions about the gauge configurations that determine the nature of dense strongly interacting matter.

While optimal, the "sign-quenched" theory that one has to simulate in the sign-reweighting approach is unfortunately not a local field theory, so the standard algorithms of lattice QCD do not apply. This leads to more costly numerics and has prevented so far the use of sign reweighting in large scale simulations on fine lattices. The state of the art so far was the study on toy lattices of Ref. [75]. After further optimization, here we demonstrate that sign reweighting has become viable for phenomenologically relevant lattices. We perform simulations of the sign-quenched theory with 2-stout improved staggered fermions at $N_\tau = 6$—a lattice action that is often used (at zero or imaginary chemical potential) as the first point of the continuum extrapolation for thermodynamic quantities [4,24,30,76–82]. We therefore obtain results directly (up to reweighting by a sign) at a finite real chemical potential, up to a baryochemical potential-temperature ratio of $\hat{\mu}_B = \frac{\mu_B}{T} = 2.7$, which is near the upper end of the chemical potential range of the Relativistic Heavy Ion Collider (RHIC) Beam Energy Scan [83–85] and is already in a region of the phase diagram where analytic continuation methods stop being predictive. Beyond previous results on toy lattices, this is the first result in the literature obtained at real baryon density without any of the unknown systematic uncertainties, such as those coming from the overlap problem and analytic continuation. To aid further studies of this kind, we also provide a way to estimate the severity of the sign problem—the main bottleneck for sign-reweighting studies—based on susceptibility measurements at $\mu_B = 0$.

II. OVERLAP PROBLEM AND SIGN REWEIGHTING

A generic reweighting method reconstructs expectation values in a desired target theory, with microscopic variables U, path integral weights $w_t(U)$, and partition function $Z_t = \int \mathcal{D}U w_t(U)$, using simulations in a theory with real and positive path integral weights $w_s(U)$ and partition function $Z_s = \int \mathcal{D}U w_s(U)$, via the formula

$$\langle \mathcal{O} \rangle_t = \frac{\left\langle \frac{w_t}{w_s} \mathcal{O} \right\rangle_s}{\left\langle \frac{w_t}{w_s} \right\rangle_s}, \quad \langle \mathcal{O} \rangle_x = \frac{1}{Z_x} \int \mathcal{D}U w_x(U) \mathcal{O}(U), \quad (1)$$

where x may stand for t or s. When the target theory is lattice QCD at finite chemical potential, the target weights $w_t(U)$ have wildly fluctuating phases; this is the infamous sign problem of lattice QCD. In addition to this problem, generic reweighting methods also suffer from an overlap problem: the probability distribution of the reweighting factor w_t/w_s has generally a long tail, which cannot be sampled efficiently in standard Monte Carlo simulations. It is actually the overlap problem, rather than the sign problem, that constitutes the immediate bottleneck in QCD when one tries to extend reweighting results to finer lattices [86].

A way to address the overlap problem is to simulate an ensemble where w_t/w_s takes values from a compact space, such as the phase-quenched [87,88] or sign-quenched [69–75] ensembles. We pursue the second approach, with a weaker sign problem. First, note that the partition function of lattice QCD is real due to charge conjugation invariance, and at finite temperature T and finite real quark chemical potential μ, one can write

$$Z(T,\mu) = \int \mathcal{D}U \,\mathrm{Re}\,\det M(U,\mu) e^{-S_g(U)}, \quad (2)$$

where S_g is the gauge action, $\det M$ denotes the fermionic determinant, including all quark types with their respective mass terms, as well as rooting in the case of staggered fermions, and the integral is over all link variables U. Replacing the determinant with its real part is not permitted for arbitrary expectation values, but it is allowed for observables satisfying $\mathcal{O}(U^*) = \mathcal{O}(U)$, as well as for those obtained as derivatives of Z with respect to real parameters, such as the chemical potential or the quark mass. As most important observables in bulk thermodynamics are of this kind, one can use Eq. (2) as the starting point for a reweighting scheme. Denoting by ε the sign of $\mathrm{Re}\,\det M(U,\mu)$, one has

$$
\begin{aligned}
Z(T,\mu) &= \langle \varepsilon \rangle^{\mathrm{SQ}}_{T,\mu} Z_{\mathrm{SQ}}(T,\mu), \\
Z_{\mathrm{SQ}}(T,\mu) &= \int \mathcal{D}U |\mathrm{Re}\det M(U,\mu)| e^{-S_g(U)}, \\
\langle \mathcal{O} \rangle^{\mathrm{SQ}}_{T,\mu} &= \frac{1}{Z_{\mathrm{SQ}}(T,\mu)} \int \mathcal{D}U \mathcal{O}(U) |\mathrm{Re}\det M(U,\mu)| e^{-S_g(U)}.
\end{aligned}
\tag{3}
$$

Here, SQ stands for sign quenched, and Z_{SQ} defines the "sign-quenched ensemble." The desired expectation values are then obtained by setting $w_s = |\mathrm{Re}\ \det\ M(U,\mu)| e^{-S_g(U)}$, $w_t = \mathrm{Re}\ \det\ M(U,\mu) e^{-S_g(U)}$, and $w_t/w_s = \varepsilon$ in Eq. (1). Since $\varepsilon = \pm 1$, reweighting boils down to a sign factor, and one avoids the problem of inaccurate sampling of the tails of the probability distribution of the reweighting factor (i.e., the overlap problem), since the tails are absent by construction. The only problem left is the sign problem, which is under control as long as $\langle \varepsilon \rangle^{\mathrm{SQ}}_{T,\mu}$ is safely not zero within errors. In this case, sign reweighting gives reliable results, and unlike any other of the commonly used methods for μ_B, error bars (for a fixed lattice setup) are statistical only.

III. SEVERITY OF THE SIGN PROBLEM

A key step in addressing the feasibility of our approach is estimating the severity of the sign problem. The sign-reweighting approach is closely related to the better known phase-reweighting approach [87,88], where in Eq. (1) we have $w_t = \det M(U,\mu) e^{-S_g(U)}$ and $w_s = |\det M(U,\mu)| e^{-S_g(U)}$, which defines the phase-quenched ensemble PQ. In the sign-quenched ensemble, the severity of the sign problem is measured by the average phase factor $\langle e^{i\theta} \rangle^{\mathrm{PQ}}_{T,\mu} = \langle \cos\theta \rangle^{\mathrm{PQ}}_{T,\mu}$, while in the sign quenched (SQ) ensemble, it is measured by $\langle \varepsilon \rangle^{\mathrm{SQ}}_{T,\mu} = \langle \cos\theta \rangle^{\mathrm{PQ}} / \langle |\cos\theta| \rangle^{\mathrm{PQ}}$. Clearly, $\langle \cos\theta \rangle^{\mathrm{PQ}}_{T,\mu} \leq \langle \varepsilon \rangle^{\mathrm{SQ}}_{T,\mu}$, so the sign problem is generally weaker in the SQ case. Moreover, the probability distribution of the phases $\theta = \arg\ \det\ M$ in the phase-quenched theory, $P_{\mathrm{PQ}}(\theta)$, controls the strength of the sign problem in both ensembles. A simple quantitative estimate can then be obtained with the following two-step approximation: (*i*) in a leading order cumulant expansion, $P_{\mathrm{PQ}}(\theta)$ is assumed to be a wrapped Gaussian distribution, and (*ii*) the chemical potential dependence of its width is approximated by the leading order Taylor expansion, $\sigma(\mu)^2 \approx \langle \theta^2 \rangle_{\mathrm{LO}} = -\frac{4}{9} \chi^{ud}_{11} (LT)^3 \hat{\mu}_B^2$ [36], where $\chi^{ud}_{11} = \frac{1}{T^2} \frac{\partial^2 p}{\partial \mu_u \partial \mu_d}|_{\mu_u = \mu_d = 0}$ is the disconnected part of the light quark susceptibility, obtained in $\mu = 0$ simulations. In this approximation, both cases can be calculated analytically, with $\langle \cos\theta \rangle^{\mathrm{PQ}}_{T,\mu} \approx e^{-\frac{\sigma^2(\mu)}{2}}$ in the phase-quenched case, while in the sign-quenched case the expression for $\langle \varepsilon \rangle^{\mathrm{SQ}}_{T,\mu}$ is more involved. It is worth noting the different asymptotics of the two cases. The small-μ (i.e., small-σ) asymptotics are notably very different, with $\langle \cos\theta \rangle^{\mathrm{PQ}}_{T,\mu} \sim 1 - \frac{\sigma^2(\mu)}{2}$ analytic in $\hat{\mu}_B$, while in the sign-quenched case $\langle \varepsilon \rangle^{\mathrm{SQ}}_{T,\mu}$ is not analytic,

$$
\langle \varepsilon \rangle^{\mathrm{SQ}}_{T,\mu} \underset{\hat{\mu}_B \to 0}{\sim} 1 - \left(\frac{4}{\pi} \right)^{\frac{5}{2}} \left(\frac{\sigma^2(\mu)}{2} \right)^{\frac{3}{2}} e^{-\frac{\pi^2}{8\sigma^2(\mu)}},
\tag{4}
$$

approaching 1 faster than any polynomial (see the Supplemental Material [89] for a derivation). The large-μ or large volume asymptotics are, on the other hand, quite similar; in the large-σ limit, a wrapped Gaussian tends to the uniform distribution, and so at large chemical potential or volume, one arrives at

$$
\frac{\langle \varepsilon \rangle^{\mathrm{SQ}}_{T,\mu}}{\langle \cos\theta \rangle^{\mathrm{PQ}}_{T,\mu}} \underset{\hat{\mu}_B \text{ or } V \to \infty}{\sim} \left(\int_{-\pi}^{\pi} d\theta |\cos\theta| \right)^{-1} = \frac{\pi}{2},
\tag{5}
$$

which asymptotically translates to a factor of $(\frac{\pi}{2})^2 \approx 2.5$ fewer statistics needed for a sign-quenched as compared to a phase-quenched simulation.

We compare our Gaussian model with simulation results for both the sign-reweighting and phase-reweighting approach in Fig. 1. Error bars on the model come solely from the statistical errors of χ^{ud}_{11} at $\mu_B = 0$. Our model describes reasonably well our simulation data at small μ in both cases, deviating less than 1σ from the actual measured strength of the sign problem up to $\hat{\mu}_B = 2$. While deviations are visible at larger μ, even at the upper end of our $\hat{\mu}_B$ range, the deviation is at most 25%, and Eq. (5) approximates well the relative severity of the sign problem in the two ensembles at $\hat{\mu}_B > 1.5$.

In summary, this shows that we can estimate the severity of the sign problem using $\mu_B = 0$ simulations only, making the planning of such reweighting studies practical. Furthermore, we have also demonstrated—using simulations at real chemical potential—that at an aspect ratio of $LT \approx 2.7$ the sign problem is manageable up to $\hat{\mu}_B = 2.7$. Covering the range of the RHIC Beam Energy Scan is therefore feasible.

IV. SIMULATION SETUP

We simulated the sign-quenched ensemble using $2+1$ flavors of rooted staggered fermions. We used a tree-level Symanzik improved gauge action, and two steps of stout smearing [95] with $\rho = 0.15$ on the gauge links fed into the fermion determinant, with physical quark masses, using the kaon decay constant f_K for scale setting (see Ref. [96] for details). We studied $16^3 \times 6$ lattices at various temperatures T and light-quark chemical potential $\mu_u = \mu_d = \mu_l = \mu = \mu_B/3$ with a zero strange quark chemical potential $\mu_s = 0$, corresponding to a strangeness chemical potential [42,97] $\mu_S = \mu_B/3$. We performed a scan in chemical potential at fixed $T = 140$ MeV and a scan in temperature at fixed $\hat{\mu}_B = 1.5$. Simulations were performed by modifying the

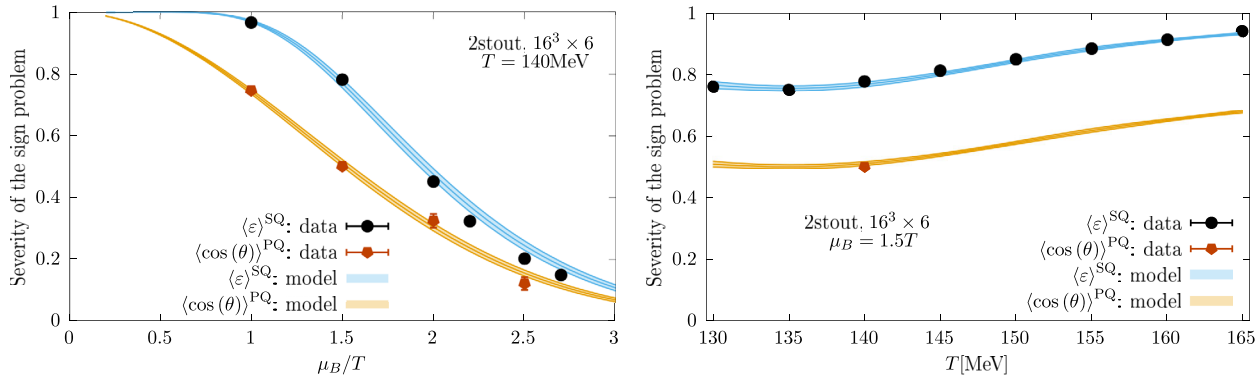

FIG. 1. The strength of the sign problem as a function of μ_B/T at $T = 140$ MeV (left) and as a function of T at $\mu_B/T = 1.5$. A value close to 1 shows a mild sign problem. A small value indicates a severe sign problem. Data for sign reweighting (black) and phase reweighting (orange) are from direct simulations. Predictions of the Gaussian model are also shown.

RHMC algorithm at $\mu_B = 0$ by including an extra accept/reject step that takes into account the factor $\frac{|\mathrm{Re\ det}\ M(\mu)|}{\det M(0)}$. The determinant was calculated with the reduced matrix formalism [49] and dense linear algebra, with no stochastic estimators involved. See the Supplemental Material [89] for a complete description of the simulation algorithm.

V. OBSERVABLES

We now proceed to display physics results. The light-quark chiral condensate was obtained via the formula

$$\langle\bar{\psi}\psi\rangle_{T,\mu} = \frac{1}{Z(T,\mu)}\frac{\partial Z(T,\mu)}{\partial m_{ud}} = \frac{T}{V}\frac{1}{\langle\varepsilon\rangle^{\mathrm{SQ}}_{T,\mu}}\left\langle\varepsilon\frac{\partial}{\partial m_{\mathrm{ud}}}\ln|\mathrm{Re\ det}\ M|\right\rangle^{\mathrm{SQ}}_{T,\mu}, \quad (6)$$

with the determinant $\det M = \det M(U, m_{ud}, m_s, \mu)$ calculated in the reduced matrix formalism at different light-quark masses and fed into a symmetric difference, $\frac{df(m)}{dm} \approx \frac{f(m+\Delta m)-f(m-\Delta m)}{2\Delta m}$, choosing Δm small enough to make the systematic error from the finite difference negligible compared to the statistical error. The renormalized condensate was obtained with the prescription

$$\langle\bar{\psi}\psi\rangle_R(T,\mu) = -\frac{m_{ud}}{f_\pi^4}[\langle\bar{\psi}\psi\rangle_{T,\mu} - \langle\bar{\psi}\psi\rangle_{0,0}]. \quad (7)$$

We also calculated the light quark density

$$\chi_1^l \equiv \frac{\partial(p/T^4)}{\partial(\mu/T)} = \frac{1}{VT^3}\frac{1}{Z(T,\mu)}\frac{\partial Z(T,\mu)}{\partial\hat{\mu}} = \frac{1}{VT^3\langle\varepsilon\rangle^{\mathrm{SQ}}_{T,\mu}}\left\langle\varepsilon\frac{\partial}{\partial\hat{\mu}}\ln|\mathrm{Re\ det}\,M|\right\rangle^{\mathrm{SQ}}_{T,\mu}, \quad (8)$$

evaluating the derivative analytically using the reduced matrix formalism (see the Supplemental Material [89]).

VI. TEMPERATURE SCAN

Our results for a temperature scan between 130 and 165 MeV at real chemical potential $\hat{\mu}_B = 1.5$, zero chemical potential, and imaginary chemical potential $\hat{\mu}_B = 1.5i$ are shown in Fig. 2. The most important quantitative question one can address with such a temperature scan is the strength of the crossover transition. Methods based on analytic continuation cannot address this particular issue efficiently. It was in fact demonstrated by numerical simulations that for imaginary chemical potentials the strength of the transition is to a good approximation constant [14,34]. However, the extrapolation of such a behavior to real chemical potentials is inherently dangerous. It is usually assumed that the transition at physical masses and $\mu_B = 0$ is close to the O(4) scaling regime in the continuum theory [2,98–101] (or O(2) with staggered fermions on the lattice [102]), while close to the critical end point, one expects to see $\mathbb{Z}_2$ scaling. One then cannot assess at what point one enters the $\mathbb{Z}_2$ region using gauge configurations that are only sensitive to O(4) [or O(2)] criticality, and extrapolations from such configurations are very likely to miss a transition to the other regime—even if it exists. Our results, however, show that the transition is not getting any stronger up to $\hat{\mu}_B = 1.5$, as convincingly demonstrated by the collapse plot in the inset of Fig. 2. In fact, data at $\hat{\mu}_B = 0, 1.5, 1.5i$ are all reasonably well described by one and the same function of $T(1 + \kappa\hat{\mu}_B^2)$.

VII. CHEMICAL POTENTIAL SCAN

Our results for the chemical potential scan at a fixed temperature of $T = 140$ MeV are shown in Fig. 3. We have performed simulations at $\hat{\mu}_B = 1$, 1.5, 2, 2.2, 2.5, 2.7. The point at $\hat{\mu}_B = 2.2$ corresponds roughly to the chiral transition, as at this point the chiral condensate is close to its value at the $\mu_B = 0$ crossover.

The sign-quenched results are compared with the analytic continuation from imaginary chemical potential results, obtained by extrapolating suitable fits to the

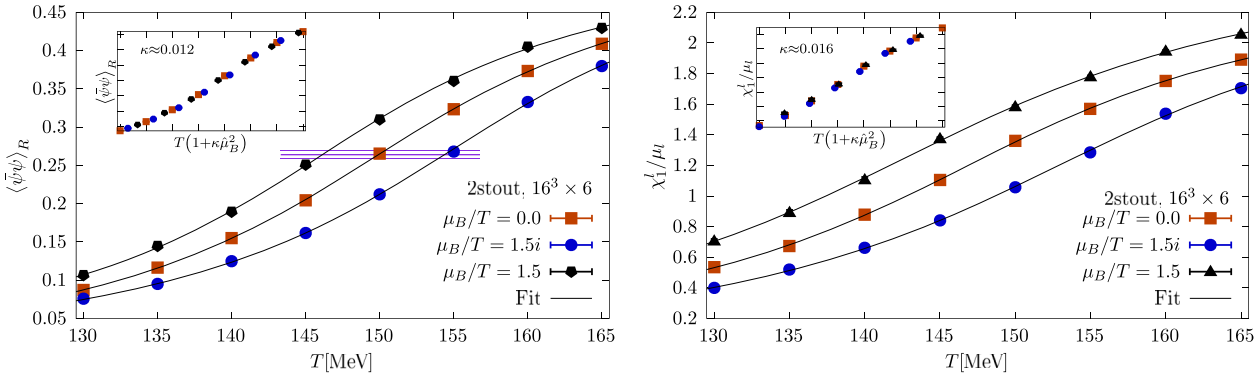

FIG. 2. The renormalized chiral condensate (left) and the light quark number-to-light quark chemical potential ratio (right) as a function of temperature at $\mu_B/T = 1.5$. The data points are shown together with an arcotangent based fit. In the insets, collapse plots are shown in the variable $T \cdot (1 + \kappa(\frac{\mu_B}{T})^2)$, with $\kappa \approx 0.012$ for the chiral condensate and $\kappa \approx 0.016$ for the quark number. In the left panel, the value of the condensate at the crossover temperature at $\mu_B = 0$ is also shown.

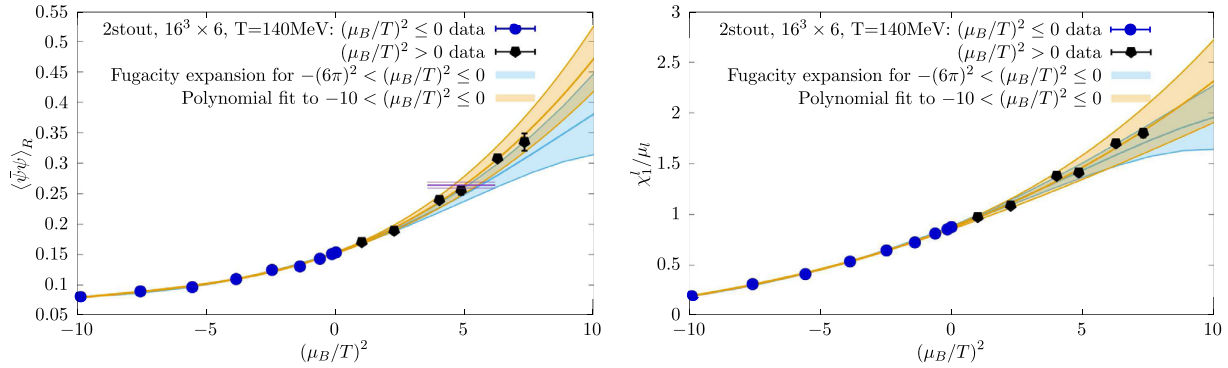

FIG. 3. The renormalized chiral condensate (left) and the light quark number-to-light quark chemical potential ratio (right) as a function of $(\mu_B/T)^2$ at temperature $T = 140$ MeV. Data from simulations at real μ_B (black) are compared with analytic continuation from imaginary μ_B (blue). In the left panel, the value of the condensate at the crossover temperature at $\mu_B = 0$ is also shown. The simulation data cross this line at $\mu_B/T \approx 2.2$.

imaginary-μ_B data from negative to positive $\hat{\mu}_B^2$. We considered two types of fits: (*i*) As the simplest Ansatz, we fitted the data with a cubic polynomial in $\hat{\mu}_B^2$ in the range $\hat{\mu}_B^2 \in [-10, 0]$. (*ii*) As an alternative, we also used suitable Ansätze for $\langle\bar{\psi}\psi\rangle_R$ condensate and $\chi_1^l/\hat{\mu}_l$ based on the fugacity expansion $p/T^4 = \sum_n A_n \cosh(n\hat{\mu})$, fitting the data in the entire imaginary-potential range $\hat{\mu}_B^2 \in [-(6\pi)^2, 0]$ using, respectively, seven and six fitting parameters. Fit results are also shown in Fig. 3; only statistical errors are displayed. While sign reweighting and analytic continuation give compatible results, at the upper half of the μ_B range, the errors from sign reweighting are an order of magnitude smaller. In fact, sign reweighting can penetrate the region $\hat{\mu}_B > 2$ where the extrapolation of many quantities is not yet possible [14,46].

VIII. CONCLUSIONS

We have demonstrated that sign reweighting has become a viable approach to finite-density lattice QCD. This is the first lattice study performed with a phenomenologically relevant lattice action (2-stout improved staggered fermions, six time slices, aspect ratio $LT \approx 2.7$) that does not require analytic continuation, unlike the Taylor expansion and imaginary μ_B methods, and is free from the overlap problem of more traditional reweighting approaches. We also presented a way to estimate the severity of the sign problem from $\mu_B = 0$ simulations, making the method practical; the computational cost for a given μ_B and a given lattice action is now easily predictable.

Note that the phase- and sign-reweighting approaches only guarantee the absence of heavy tailed distributions when calculating the ratio of the partition functions (or the pressure difference) of the target and simulated theories. We leave the study of the probability distributions of other observables to future work.

Our temperature scan at $\mu_B/T = 1.5$ shows no sign of the transition getting stronger. Furthermore, while the results of the μ_B scan at $T = 140$ MeV are compatible with those obtained from extrapolation from imaginary μ_B, the errors of the sign-reweighting method are an order of magnitude

smaller, opening up new possibilities. Our chemical potential scan shows that small statistical errors can be achieved up to $\mu_B/T = 2.7$, and our temperature scan shows that the severity of the sign problem is only weakly dependent on the temperature (Fig. 1, right). Our method is then optimized enough to make a full scan of the chiral transition region in the RHIC Beam Energy Scan range feasible, with computing resources available today. Such a scan allows us to attack the most important open question of the Beam Energy Scan and decide whether the crossover transition becomes stronger in the range, as expected for a nearby critical end point [84,85,103–106]. It would also allow us to obtain the equation of state directly and test the range of validity of several recently proposed resummation schemes [34,107] for the Taylor expansion of the pressure in μ_B.

The lattice action used in this study is often the first point of a continuum extrapolation in QCD thermodynamics. Furthermore, while the sign problem is exponential in the physical volume, it is not so in the lattice spacing. Continuum-extrapolated finite μ_B results in the range of the RHIC Beam Energy Scan are then almost within reach for the phenomenologically relevant aspect ratio of $LT \approx 3$. On the theoretical side, sampling the most relevant configurations allows one to study detailed aspects of the theory at $\mu_B > 0$, such as spectral statistics of the Dirac operator, likely leading to new insights.

ACKNOWLEDGMENTS

We thank Tamás G. Kovács for useful discussions. The project was supported by the BMBF Grant No. 05P18PXFCA. This work was also supported by the Hungarian National Research, Development and Innovation Office, NKFIH Grant No. KKP126769. A. P. is supported by the J. Bolyai Research Scholarship of the Hungarian Academy of Sciences and by the ÚNKP-20-5 New National Excellence Program of the Ministry for Innovation and Technology. The authors gratefully acknowledge the Gauss Centre for Supercomputing e.V. (www.gauss-centre.eu) for funding this project by providing computing time on the GCS Supercomputers JUWELS/Booster and JURECA/Booster at FZ-Juelich.

[1] N. Cabibbo and G. Parisi, Phys. Lett. **59B**, 67 (1975).
[2] R. D. Pisarski and F. Wilczek, Phys. Rev. D **29**, 338 (1984).
[3] P. Gerber and H. Leutwyler, Nucl. Phys. **B321**, 387 (1989).
[4] Y. Aoki, G. Endrődi, Z. Fodor, S. D. Katz, and K. K. Szabó, Nature (London) **443**, 675 (2006).
[5] Sz. Borsányi, Z. Fodor, C. Hoelbling, S. D. Katz, S. Krieg, C. Ratti, and K. K. Szabó (Wuppertal-Budapest Collaboration), J. High Energy Phys. 09 (2010) 073.
[6] A. Bazavov *et al.*, Phys. Rev. D **85**, 054503 (2012).
[7] K. Fukushima, Phys. Rev. D **77**, 114028 (2008); **78**, 039902(E) (2008).
[8] P. Kovács, Zs. Szép, and G. Wolf, Phys. Rev. D **93**, 114014 (2016).
[9] P. Isserstedt, M. Buballa, C. S. Fischer, and P. J. Gunkel, Phys. Rev. D **100**, 074011 (2019).
[10] F. Gao and J. M. Pawlowski, Phys. Lett. B **820**, 136584 (2021).
[11] A. Bazavov *et al.* (HotQCD Collaboration), Phys. Lett. B **795**, 15 (2019).
[12] H. T. Ding, P. Hegde, O. Kaczmarek, F. Karsch, A. Lahiri, S.-T. Li, S. Mukherjee, H. Ohno, P. Petreczky, C. Schmidt, and P. Steinbrecher (HotQCD Collaboration), Phys. Rev. Lett. **123**, 062002 (2019).
[13] N. Haque and M. Strickland, Phys. Rev. C **103**, L031901 (2021).
[14] Sz. Borsányi, Z. Fodor, J. N. Günther, R. Kara, S. D. Katz, P. Parotto, A. Pásztor, C. Ratti, and K. K. Szabó, Phys. Rev. Lett. **125**, 052001 (2020).
[15] A. Y. Kotov, M. P. Lombardo, and A. Trunin, Phys. Lett. B **823**, 136749 (2021).
[16] G. Kovács, P. Kovács, and Zs. Szép, Phys. Rev. D **104**, 056013 (2021).
[17] I. Montvay and G. Münster, *Quantum Fields on a Lattice, Cambridge Monographs on Mathematical Physics* (Cambridge University Press, Cambridge, England, 1997).
[18] P. de Forcrand and O. Philipsen, Nucl. Phys. **B642**, 290 (2002).
[19] M. D'Elia and M. P. Lombardo, Phys. Rev. D **67**, 014505 (2003).
[20] M. D'Elia and F. Sanfilippo, Phys. Rev. D **80**, 014502 (2009).
[21] P. Cea, L. Cosmai, and A. Papa, Phys. Rev. D **89**, 074512 (2014).
[22] C. Bonati, P. de Forcrand, M. D'Elia, O. Philipsen, and F. Sanfilippo, Phys. Rev. D **90**, 074030 (2014).
[23] P. Cea, L. Cosmai, and A. Papa, Phys. Rev. D **93**, 014507 (2016).
[24] C. Bonati, M. D'Elia, M. Mariti, M. Mesiti, F. Negro, and F. Sanfilippo, Phys. Rev. D **92**, 054503 (2015).
[25] R. Bellwied, S. Borsányi, Z. Fodor, J. Günther, S. D. Katz, C. Ratti, and K. K. Szabó, Phys. Lett. B **751**, 559 (2015).
[26] M. D'Elia, G. Gagliardi, and F. Sanfilippo, Phys. Rev. D **95**, 094503 (2017).
[27] J. N. Günther, R. Bellwied, S. Borsányi, Z. Fodor, S. D. Katz, A. Pásztor, C. Ratti, and K. K. Szabó, Proceedings of the 26th International Conference on Ultra-relativistic Nucleus-Nucleus Collisions (Quark Matter 2017): Chicago, Illinois, USA, 2017 [*Nucl. Phys.* A967, 720 (2017)].
[28] P. Alba *et al.*, Phys. Rev. D **96**, 034517 (2017).
[29] V. Vovchenko, A. Pásztor, Z. Fodor, S. D. Katz, and H. Stoecker, Phys. Lett. B **775**, 71 (2017).

[30] C. Bonati, M. D'Elia, F. Negro, F. Sanfilippo, and K. Zambello, Phys. Rev. D **98**, 054510 (2018).
[31] Sz. Borsányi, Z. Fodor, J. N. Günther, S. K. Katz, K. K. Szabó, A. Pásztor, I. Portillo, and C. Ratti, J. High Energy Phys. 10 (2018) 205.
[32] R. Bellwied, Sz. Borsányi, Z. Fodor, J. N. Günther, J. Noronha-Hostler, P. Parotto, A. Pásztor, C. Ratti, and J. M. Stafford, Phys. Rev. D **101**, 034506 (2020).
[33] A. Pásztor, Zs. Szép, and G. Markó, Phys. Rev. D **103**, 034511 (2021).
[34] S. Borsányi, Z. Fodor, J. N. Günther, R. Kara, S. D. Katz, P. Parotto, A. Pásztor, C. Ratti, and K. K. Szabó, Phys. Rev. Lett. **126**, 232001 (2021).
[35] R. Bellwied, Sz. Borsányi, Z. Fodor, J. N. Guenther, S. D. Katz, P. Parotto, A. Pásztor, D. Pesznyák, C. Ratti, and K. K. Szabó, Phys. Rev. D **104**, 094508 (2021).
[36] C. R. Allton, S. Ejiri, S. J. Hands, O. Kaczmarek, F. Karsch, E. Laermann, C. Schmidt, and L. Scorzato, Phys. Rev. D **66**, 074507 (2002).
[37] R. V. Gavai and S. Gupta, Phys. Rev. D **68**, 034506 (2003).
[38] R. V. Gavai and S. Gupta, Phys. Rev. D **71**, 114014 (2005).
[39] C. R. Allton, M. Doring, S. Ejiri, S. J. Hands, O. Kaczmarek, F. Karsch, E. Laermann, and K. Redlich, Phys. Rev. D **71**, 054508 (2005).
[40] R. V. Gavai and S. Gupta, Phys. Rev. D **78**, 114503 (2008).
[41] S. Basak *et al.* (MILC Collaboration), Proc. Sci., LATTICE2008 (**2008**) 171 [arXiv:0910.0276].
[42] Sz. Borsányi, Z. Fodor, S. D. Katz, S. Krieg, C. Ratti, and K. Szabó, J. High Energy Phys. 01 (2012) 138.
[43] S. Borsányi, G. Endrődi, Z. Fodor, S. Katz, S. Krieg, C. Ratti, and K. K. Szabó, J. High Energy Phys. 08 (2012) 053.
[44] R. Bellwied, S. Borsányi, Z. Fodor, S. D. Katz, A. Pásztor, C. Ratti, and K. K. Szabó, Phys. Rev. D **92**, 114505 (2015).
[45] H. T. Ding, S. Mukherjee, H. Ohno, P. Petreczky, and H. P. Schadler, Phys. Rev. D **92**, 074043 (2015).
[46] A. Bazavov *et al.*, Phys. Rev. D **95**, 054504 (2017).
[47] M. Giordano and A. Pásztor, Phys. Rev. D **99**, 114510 (2019).
[48] A. Bazavov *et al.*, Phys. Rev. D **101**, 074502 (2020).
[49] A. Hasenfratz and D. Toussaint, Nucl. Phys. **B371**, 539 (1992).
[50] I. M. Barbour, S. E. Morrison, E. G. Klepfish, J. B. Kogut, and M.-P. Lombardo, Nucl. Phys. B Proc. Suppl.**60**, 220 (1998).
[51] Z. Fodor and S. D. Katz, Phys. Lett. B **534**, 87 (2002).
[52] Z. Fodor and S. D. Katz, J. High Energy Phys. 03 (2002) 014.
[53] Z. Fodor and S. D. Katz, J. High Energy Phys. 04 (2004) 050.
[54] M. Giordano, K. Kapás, S. D. Katz, D. Nógrádi, and A. Pásztor, Phys. Rev. D **101**, 074511 (2020).
[55] E. Seiler, D. Sexty, and I.-O. Stamatescu, Phys. Lett. B **723**, 213 (2013).
[56] D. Sexty, Phys. Lett. B **729**, 108 (2014).
[57] G. Aarts, E. Seiler, D. Sexty, and I.-O. Stamatescu, Phys. Rev. D **90**, 114505 (2014).
[58] Z. Fodor, S. D. Katz, D. Sexty, and C. Török, Phys. Rev. D **92**, 094516 (2015).
[59] D. Sexty, Phys. Rev. D **100**, 074503 (2019).
[60] J. B. Kogut and D. K. Sinclair, Phys. Rev. D **100**, 054512 (2019).
[61] M. Scherzer, D. Sexty, and I. O. Stamatescu, Phys. Rev. D **102**, 014515 (2020).
[62] C. Gattringer, Proc. Sci., LATTICE2013 (**2014**) 002 [arXiv:1401.7788].
[63] C. Marchis and C. Gattringer, Phys. Rev. D **97**, 034508 (2018).
[64] M. Cristoforetti, F. Di Renzo, and L. Scorzato (AuroraScience Collaboration), Phys. Rev. D **86**, 074506 (2012).
[65] M. Cristoforetti, F. Di Renzo, A. Mukherjee, and L. Scorzato, Phys. Rev. D **88**, 051501 (2013).
[66] A. Alexandru, G. Başar, and P. Bedaque, Phys. Rev. D **93**, 014504 (2016).
[67] A. Alexandru, G. Başar, P. F. Bedaque, G. W. Ridgway, and N. C. Warrington, Phys. Rev. D **93**, 094514 (2016).
[68] J. Nishimura and S. Shimasaki, J. High Energy Phys. 06 (2017) 023.
[69] P. de Forcrand, S. Kim, and T. Takaishi, Nucl. Phys. B Proc. Suppl. **119**, 541 (2003).
[70] P. de Forcrand, Proc. Sci., LAT2009 (**2009**) 010.
[71] S. D. H. Hsu and D. Reeb, Int. J. Mod. Phys. A **25**, 53 (2010).
[72] A. Alexandru, M. Faber, I. Horváth, and K.-F. Liu, Phys. Rev. D **72**, 114513 (2005).
[73] A. Li, A. Alexandru, K.-F. Liu, and X. Meng, Phys. Rev. D **82**, 054502 (2010).
[74] A. Li, A. Alexandru, and K.-F. Liu, Phys. Rev. D **84**, 071503 (2011).
[75] M. Giordano, K. Kapás, S. D. Katz, D. Nógrádi, and A. Pásztor, J. High Energy Phys. 05 (2020) 088.
[76] Y. Aoki, Z. Fodor, S. D. Katz, and K. K. Szabó, Phys. Lett. B **643**, 46 (2006).
[77] Sz. Borsányi, G. Endrődi, Z. Fodor, A. Jakovác, S. D. Katz, S. Krieg, C. Ratti, and K. K. Szabó, J. High Energy Phys. 11 (2010) 077.
[78] G. S. Bali, F. Bruckmann, G. Endrődi, Z. Fodor, S. D. Katz, S. Krieg, A. Schäfer, and K. K. Szabó, J. High Energy Phys. 02 (2012) 044.
[79] G. S. Bali, F. Bruckmann, G. Endrődi, Z. Fodor, S. D. Katz, and A. Schäfer, Phys. Rev. D **86**, 071502 (2012).
[80] Sz. Borsányi, Z. Fodor, S. D. Katz, A. Pásztor, K. K. Szabó, and Cs. Török, J. High Energy Phys. 04 (2015) 138.
[81] B. B. Brandt, G. Endrődi, and S. Schmalzbauer, Phys. Rev. D **97**, 054514 (2018).
[82] M. D'Elia, F. Negro, A. Rucci, and F. Sanfilippo, Phys. Rev. D **100**, 054504 (2019).
[83] L. Adamczyk *et al.* (STAR Collaboration), Phys. Rev. C **96**, 044904 (2017).
[84] A. Bzdak, S. Esumi, V. Koch, J. Liao, M. Stephanov, and N. Xu, Phys. Rep. **853**, 1 (2020).
[85] J. Adam *et al.* (STAR Collaboration), Phys. Rev. Lett. **126**, 092301 (2021).
[86] M. Giordano, K. Kapás, S. D. Katz, D. Nógrádi, and A. Pásztor, Phys. Rev. D **102**, 034503 (2020).
[87] Z. Fodor, S. D. Katz, and C. Schmidt, J. High Energy Phys. 03 (2007) 121.
[88] G. Endrődi, Z. Fodor, S. D. Katz, D. Sexty, K. K. Szabó, and C. Török, Phys. Rev. D **98**, 074508 (2018).

[89] See Supplemental Material at http://link.aps.org/supplemental/10.1103/PhysRevD.105.L051506 for a complete description of the simulation algorithm, which includes Refs. [90–94].
[90] N. I. Fisher, *Statistical Analysis of Circular Data* (Cambridge University Press, Cambridge, England, 1993).
[91] M. Abramowitz and I. A. Stegun, *Handbook of Mathematical Functions with Formulas, Graphs, and Mathematical Tables* (U.S. Government Printing Office, Washington, D.C., 1964), Vol. 55.
[92] J. B. Kogut and D. K. Sinclair, Phys. Rev. D **66**, 034505 (2002).
[93] G. H. Golub and C. F. Van Loan, *Matrix Computations*, 3rd ed. (Johns Hopkins University Press, Baltimore, 1996).
[94] S. Tomov, J. Dongarra, and M. Baboulin, Parallel Comput. **36**, 232 (2010).
[95] C. Morningstar and M. J. Peardon, Phys. Rev. D **69**, 054501 (2004).
[96] Y. Aoki, Sz. Borsányi, S. Durr, Z. Fodor, S. D. Katz, S. Krieg, and K. K. Szabó, J. High Energy Phys. 06 (2009) 088.
[97] V. Koch, A. Majumder, and J. Randrup, Phys. Rev. Lett. **95**, 182301 (2005).
[98] A. Butti, A. Pelissetto, and E. Vicari, J. High Energy Phys. 08 (2003) 029.
[99] A. Pelissetto and E. Vicari, Phys. Rev. D **88**, 105018 (2013).
[100] M. Grahl and D. H. Rischke, Phys. Rev. D **88**, 056014 (2013).
[101] Y. Nakayama and T. Ohtsuki, Phys. Rev. D **91**, 021901 (2015).
[102] G. Boyd, J. Fingberg, F. Karsch, L. Kärkkäinen, and B. Petersson, Nucl. Phys. **B376**, 199 (1992).
[103] E. Shuryak and J. M. Torres-Rincon, Phys. Rev. C **101**, 034914 (2020).
[104] E. Shuryak and J. M. Torres-Rincon, Eur. Phys. J. A **56**, 241 (2020).
[105] P. Braun-Munzinger, B. Friman, K. Redlich, A. Rustamov, and J. Stachel, Nucl. Phys. **A1008**, 122141 (2021).
[106] D. Mroczek, A. R. Nava Acuna, J. Noronha-Hostler, P. Parotto, C. Ratti, and M. A. Stephanov, Phys. Rev. C **103**, 034901 (2021).
[107] S. Mondal, S. Mukherjee, and P. Hegde, Phys. Rev. Lett. **128**, 022001 (2022).